Postprint

Access to the published version may require subscription.

N.B. When citing this work, cite the original published paper.

1   Targeted repression of essential genes to arrest growth and

2   increase carbon partitioning and biofuel titers in cyanobacteria

3

4

5   Kiyan Shabestary, Josefine Anfelt, Emil Ljungqvist, Michael Jahn, Lun Yao and Elton

6   P. Hudson*

7
8   KTH—Royal Institute of Technology.
9   School of Engineering Sciences in Chemistry, Biotechnology, and Health,
10 Science for Life Laboratory,
11 Stockholm SE-171 21 Sweden.
12
13 *Correspondence to paul.hudson@biotech.kth.se
14
15 kiyan@kth.se
16 janfelt@kth.se
17 emilel2@kth.se
18 michael.jahn@scilifelab.se
19 lunyao@kth.se
20 paul.hudson@biotech.kth.se
21

22

Graphical abstract
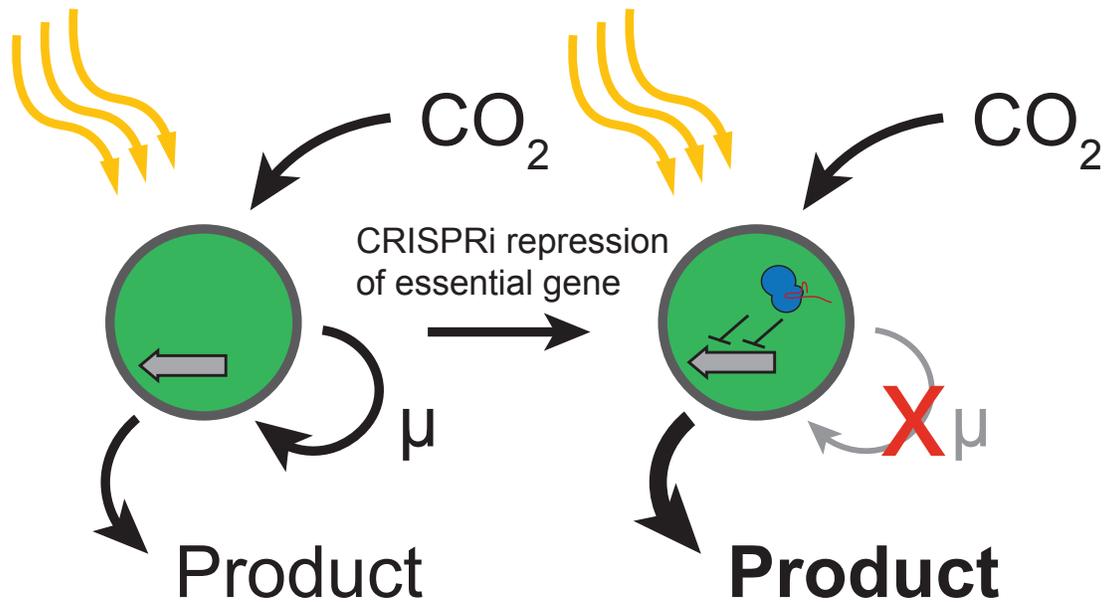
25
26
27
28
29   **Abstract**

30   Photoautotrophic production of fuels and chemicals by cyanobacteria typically gives

31   lower volumetric productivities and titers than heterotrophic production.

32   Cyanobacteria cultures become light limited above an optimal cell density, so that

33   this substrate is not supplied to all cells sufficiently. Here, we investigate genetic

34   strategies for a two-phase cultivation, where biofuel-producing *Synechocystis*

35   cultures are limited to an optimal cell density through inducible CRISPR interference

36   (CRISPRi) repression of cell growth. Fixed CO_2 is diverted to ethanol or n-butanol.

37   Among the most successful strategies was partial repression of citrate synthase *gltA.*

38   Strong repression (>90%) of *gltA* at low culture densities increased carbon

39   partitioning to n-butanol 5-fold relative to a non-repression strain, but sacrificed

40   volumetric productivity due to severe growth restriction. CO_2 fixation continued for

41   at least 3 days after growth was arrested. By targeting sgRNAs to different regions of

42   the *gltA* gene, we could modulate GltA expression and carbon partitioning between

43   growth and product to increase both specific and volumetric productivity. These

44   growth arrest strategies can be useful for improving performance of other

45   photoautotrophic processes.

46
47   **Keywords:** Dynamic metabolic engineering, Cyanobacteria, Growth-arrest, Light
48   availability, CRISPRi

49   The tradeoff between growth and specific productivity must be tightly

50   regulated when producing compounds in microbial cell factories. If carbon

51   partitioning towards product is too high, cellular density accumulates slowly,

52   resulting in low volumetric productivity. Conversely, low specific productivities

53   result in low yields since substrate is mainly converted to biomass. The ideal

54   bioprocess would be divided into two parts: rapid biomass accumulation to an

55   optimal cell density, and then rapid product synthesis with minimum or no biomass

56   formation. In dynamic metabolic engineering, carbon flux to growth and production

57   are altered during the bioprocess.[1,2] Flux alterations can be achieved by partially or

58   completely repressing enzyme levels essential for biomass formation,[3] involved in

59   glycolysis,[4–6] fatty acid synthesis (OPX Biotechnologies, US Patent application,

60   US2010/8883464), terpenoid synthesis,[7] nucleobase synthesis or cell division.[8] The

61   signal for switching between growth and production can be externally added, but is

62   ideally generated *in situ*. Photoautotrophic production processes in particular would

63   benefit from biomass repression since light shading at high cell densities can reduce

64   specific and total productivities.[9,10]

65   The CRISPR-interference (CRISPRi) system has been recently ported to

66   cyanobacteria, where it has been used to repress genes upon induction with

67   external effector molecules.[11–14] CRISPRi could thus be a useful tool for an eventual

68   two-phase cyanobacteria process. Here, we evaluate the effectiveness of CRISPRi to

69   arrest cell growth and divert fixed CO_2 to biofuel in *Synechocystis* PCC6803 strains

70   engineered to produce n-butanol and ethanol (Fig. 1). The ethanol production

71   cassette contained a copy of the native *Synechocystis* alcohol dehydrogenase

72   (*slr1192*) and a pyruvate decarboxylase (*pdc*) from *Zymomonas mobilis* (Table 1).

73   The n-butanol cassette contained a heterologous phosphoketolase (Xfpk) to increase

74   acetyl-CoA pools[15] and a heterologous acetoacetyl-CoA synthase (NphT7) to impart

75   thermodynamic driving to synthesize acetoacetyl-CoA from malonyl-CoA.[16] In an

76   ethanol-producing strain (KS33, Table S1), we repressed *odhB*, an essential subunit

77   of pyruvate dehydrogenase complex (PDH) to create KS92. PDH catalyzes the

78   decarboxylation of pyruvate and formation of acetyl-CoA. The condition-dependent

79   expression of *odhB* has been reported previously as a growth-control strategy for

80   cyanobacteria (Joule Unlimited, US Patent application, US2012/0164705). In a

81   butanol-producing strain (KS70, Table S1), we targeted citrate synthase (*gltA*) to

82   create KS96. GltA consumes acetyl-CoA in the first step of the TCA cycle, an

83   important route for α-ketoglutarate derived amino acids and other biomass

84   precursors. Modulation of *gltA* expression through heterologous promoters, RBS

85   libraries, or a protein degradation tag has been recently demonstrated to increase

86   acetyl-CoA pools and biofuel production in *E. coli.*[5,17] In addition to these specific

87   pathways, we tested repression of essential enzymes in nucleobase synthesis[8] (*pyrF*,

88   KS93 and KS162) and nitrate uptake[18] (*nrtA*, KS94) as general growth-arrest

89   strategies. All repression targets except *odhB* were confirmed as essential for

90   growth using flux balance analysis (FBA) on a genome-scale model.[19] *In silico*, the

91   native Xfpk reactions could bypass the PDH (*odhB*) knockout. *In vivo,* Xfpk could not

92   rescue the growth-defect phenotype of *odhB* repression (Fig. 2A), indicating a low

93   enzyme capacity. For each target, sgRNAs and dCas9 were under the tightly

94   repressed, anhydrotetracycline (aTc) inducible promoter PL_{22}.[20]
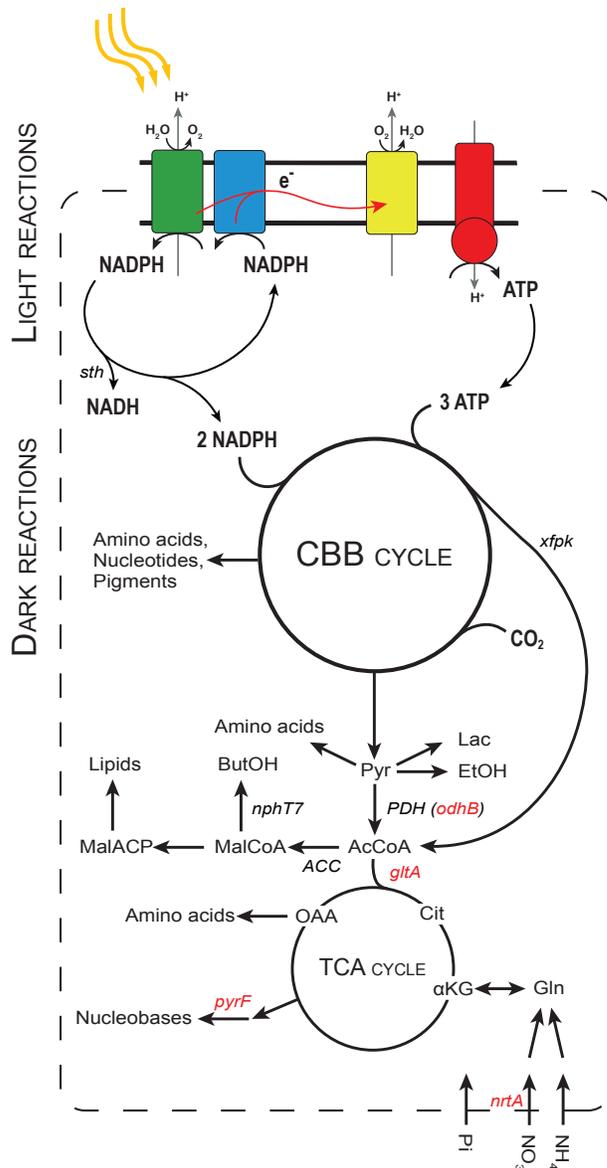
Figure 1. Simplified metabolic map of *Synechocystis* showing routes to butanol and ethanol production. Genes targeted for repression using CRISPRi in this study are indicated in red.

In first trials, CRISPRi-mediated knockdown was induced at low culture density (OD_{730} 0.1) and cultures monitored over 5 days (Fig. 2A,B). Repression of transcription of each gene was confirmed using RT-qPCR and was greater than 50% relative to non-induced cultures (Fig. S1). Repression of *gltA* (>90% repressed),
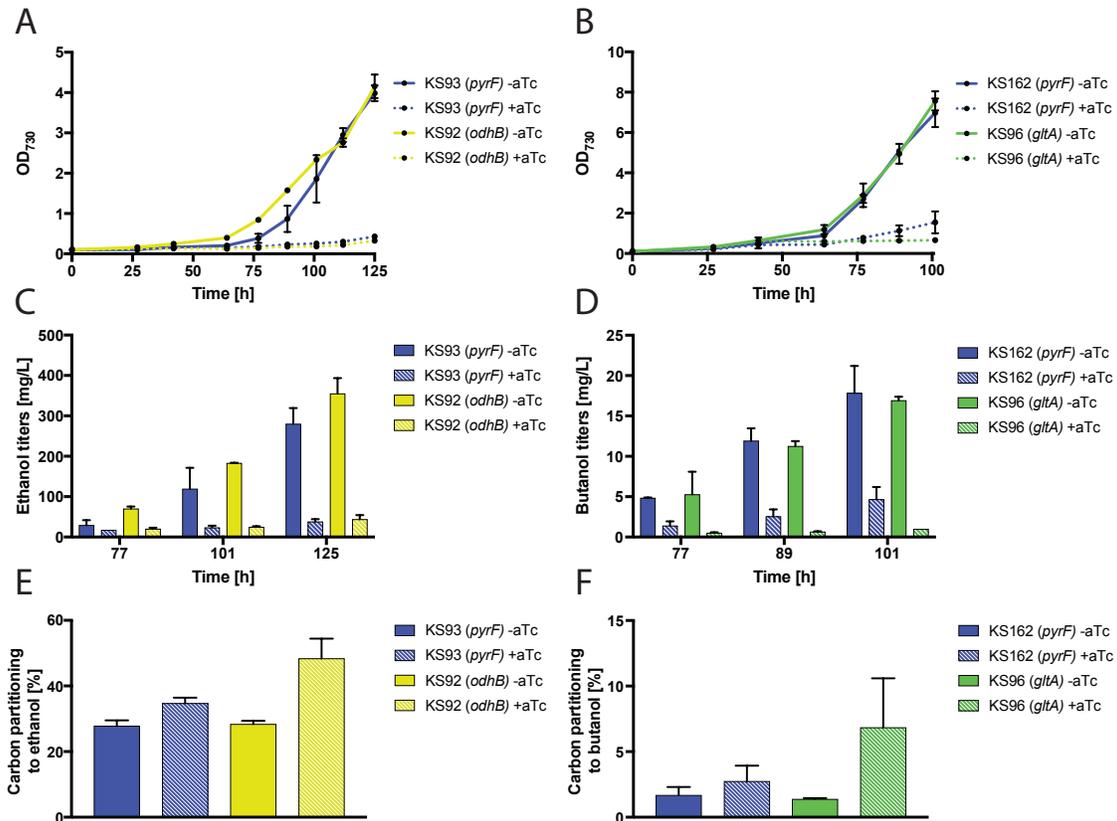
103   *odhB* (>50% repressed), and *pyrF* (>60% repressed) arrested cell growth (Fig.

104   2A,B). We also measured ethanol and butanol titers and calculated carbon

105   partitioning for the growth repression strains. In all cases, product titers and

106   specific productivities were lower when CRISPRi arrested growth due to a low cell

107   density and cessation of CO_2 uptake and possible photoinhibition (Fig. 2C,D and Fig.

108   S2). However, carbon partitioning to biofuel was higher when growth was arrested

109   in KS92 (*odhB*) and KS96 (*gltA*), though error bars were large due to variability in

110   the growth arrest (Fig. 2E,F). KS92 (*odhB*) and KS96 (*gltA*) had 2-fold and 5-fold

111   higher carbon partitioning to ethanol and butanol, respectively, when growth was

112   arrested. The strong effect from these targets is likely due to pyruvate and acetyl-

113   CoA precursor build-up, in addition to repression of biomass formation. In KS93 and

114   KS162 (*pyrF*), carbon partitioning was only mildly affected, likely because this

115   repression target is not a metabolic branch point (Fig. 2E,F). The *nrtA* repression

116   strain KS94 also had a significant increase in carbon partitioning to butanol (Fig.

117   S3). However, a chlorosis (bleached) phenotype was observed due to the onset of

118   internal nitrogen limitation, which rapidly stopped CO_2 uptake. Due to the 5-fold

119   increase in carbon partitioning to butanol in KS96, we sought to optimize the timing

120   and strength of *gltA* repression.

121

122   **Table 1.** Strains used in this study.

| Strain	Pathway cassette	dCas9 cassette		sgRNA cassette
KS92	Δslr0168::Ptrc adhA pdc KmR	ΔpsbA1::PL22 SpR	dCas9	Δslr2030-2031::PL22_sgRNA-odhB_184 odhB_318 CmR
KS93	Δslr0168::Ptrc adhA pdc KmR	ΔpsbA1::PL22 SpR	dCas9	Δslr2030-2031::PL22_sgRNA-pyrF_12 pyrF_215 CmR
KS94	Δslr0168::Ptrc pduP phaJ Ptrc ter phaB KmR, ΔphaA::Psca6-2 nphT7 xfpk GmR	ΔpsbA1::PL22 SpR	dCas9	Δslr2030-2031::PL22 sgRNA-nrtA_14 phaEC_95 CmR
KS96	Δslr0168::Ptrc pduP phaJ Ptrc ter phaB KmR, ΔphaA::Psca6-2 nphT7 xfpk GmR	ΔpsbA1::PL22 SpR	dCas9	Δslr2030-2031::PL22 sgRNA-gltA_42 gltA_164 CmR
KS162	Δslr0168::Ptrc pduP phaJ Ptrc ter phaB KmR, ΔphaA::Psca6-2 nphT7 xfpk GmR	ΔpsbA1::PL22 SpR	dCas9	Δslr2030-2031::PL22_sgRNA-pyrF_12 pyrF_215 CmR
KS87	Δslr0168::Ptrc pduP phaJ Ptrc ter phaB KmR, ΔphaA::Psca6-2 nphT7 xfpk sth GmR	ΔpsbA1::PL31 SpR	dCas9	Δslr2030-2031::PL22 sgRNA-phaE_20 ackA_95 ndhD1_134 ndhD2_39 CmR
KS142	Δslr0168::Ptrc pduP phaJ Ptrc ter phaB KmR, ΔphaA::Psca6-2 nphT7 xfpk sth GmR	ΔpsbA1::PL31 SpR	dCas9	Δslr2030-2031::PL22 sgRNA-gltA_463 ackA_21 phaEC_95 ndhD1_134 ndhD2_39 CmR
KS143	Δslr0168::Ptrc pduP phaJ Ptrc ter phaB KmR, ΔphaA::Psca6-2 nphT7 xfpk sth GmR	ΔpsbA1::PL31 SpR	dCas9	Δslr2030-2031::PL22 sgRNA-gltA_762 ackA_21 phaEC_95 ndhD1_134 ndhD2_39 CmR

123

124
125 **Figure 2.** Effect of CRISPRi-mediated gene repression on *Synechocystis* growth, titer and carbon partitioning to
126 biofuel. (A,B) Growth curves, (C,D) biofuel titers, and (E,F) average carbon partitioning to ethanol and butanol.
127 Cultures were started in flasks at OD_{730} 0.1 with or without aTc, which induced CRISPRi. Butanol production was
128 induced with IPTG at OD_{730} 0.4. Ethanol production was constitutive. Cultivations were performed in duplicate.
129 Light intensity was 100 µE. Carbon partitioning to product was calculated as the flux going to product over the
130 flux going to biomass and product in C-mol/gDCW/h (Supplementary Note).

131

132   We first aimed to increase volumetric butanol titers from KS96 by inducing

133 *gltA* repression at higher cell densities. We tested induction at OD_{730} 0.1 (12 h after

134 culture inoculation) and at OD_{730} 0.4 (18 h after). Induction at OD_{730} 0.1 prevented

135 cells from reaching a high cell density (OD_{730} < 1.0) and butanol titers were lower

136 than the non-induced culture (Fig. S4). Induction at OD_{730} 0.4 allowed cells to reach

137 higher cell density (OD_{730} 4.0), and titers were 70% higher than the non-induced

138 culture. Specific productivities also improved 2-fold (Fig. S4). These results show

139 the importance of timing the growth arrest to achieve high specific and volumetric

productivity. In a recent study, the optimal cell density for photoautotrophic production was calculated to be 0.76 gDCW/L corresponding to approximately OD_{730} 2.0.[9,15] To stop growth at the optimal cell density, one must consider the delay between CRISPRi induction and effect, as GltA protein already present in the cell must be diluted or degraded. To reduce such a delay, a protease degradation sequence could be added to GltA.[21]

One complication with a growth-arrest production strategy is that substrate uptake may be linked to growth. Growth repression due to nutrient limitation or repression of biomass formation has been shown to reduce metabolic activity in heterotrophs, often in the form of reduced glucose uptake.[6,8,22] A recent study showed decreased photosynthetic activity and ethanol production by *Synechocystis* when growth stalled in stationary phase.[10] We measured CO_2 uptake in KS96 (*gltA*) grown in a batch photobioreactor with and without growth arrest (Fig. 3A,B).[23] At the early stages of cultivation (38 h), before the onset of light limitation, the induced KS96 (*gltA*) had a higher specific CO_2-uptake rate, perhaps indicative of a sink effect on CO_2 uptake as carbon is routed to butanol.[24] At 62 h (2.5 d) post-induction, cell growth was completely arrested, though CO_2 fixation continued for at least 2 more days. At 111 h (4.5 d) post-induction, the specific CO_2 uptake rate in the growth-arrested culture had dropped to 25% of its initial value. It was clear that butanol synthesis alone could not sustain high CO_2 uptake for an extended time once growth was arrested. It is possible that an accumulation of metabolic intermediates signals CO_2 uptake to cease, or at least some flux through GltA is required to repair damaged proteins so that the metabolic rate can be maintained. One hypothesis is

164   that the cell becomes over-reduced without biomass formation as a reductant sink.

165   We measured NADPH at two time points during growth arrest and found that it was

166   at least 2-fold higher than when cells were not growth arrested (Fig. 3C). The

167   specific CO_2 uptake rate in the control culture also decreased with time, due to light

168   shading at high cell densities. We note that the volumetric CO_2 uptake rates were

169   lower in the growth-arrested culture due to a lower cell density (Fig. S5).
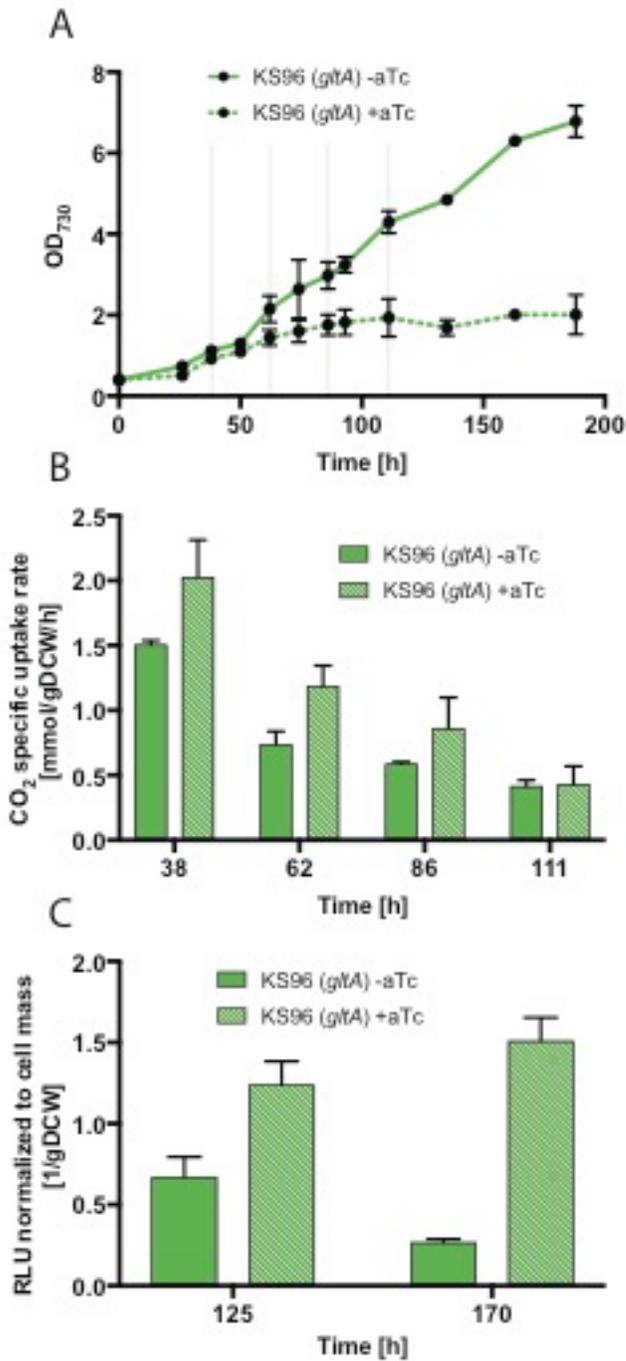
Figure 3. Growth, CO_2 uptake, and NADPH accumulation in KS96 (butanol-producing) during CRISPRi-mediated growth arrrest. Cells were grown in a batch photobioreactor. (A) Growth curve, where gray lines indicate when CO_2 uptake was measured. (B) Specific CO_2 uptake rate (biomass normalized). (C) Relative NADPH concentration as measured by luminescence assay (RLU relative light units). Cultures were inoculated at OD_{730} 0.1 in all cases. Repression of *gltA* was induced at culture start by addition of aTc. Butanol production was induced with IPTG at OD_{730} 0.4. Light intensity was 300 µE. Cultivations for CO_2 uptake rate were performed in duplicate. NADPH measurements were performed in triplicate.

180   Since strong *gltA* repression (>90% repressed) in KS96 led to total growth

181   arrest and reduced CO_2 uptake, we tested partial repression of *gltA* as a way to

182   potentially hinder growth while allowing significant CO_2 uptake*.* We designed new

183   sgRNAs that would bind the *gltA* gene far from its transcription start site (TSS),

184   resulting in different levels of *gltA* expression. The potency of gene repression by

185   dCas9-sgRNA is weakened when the sgRNA binds far from the TSS.[25] We

186   constructed sgRNA arrays containing sgRNA_*gltA*_463 (targeting 463 nt from TSS)

187   and sgRNA_*gltA*_762 (targeting 762 nt from TSS). In this trial, the arrays also

188   contained sgRNAs targeting subunits of the NAD(P)H dehydrogenase complex NDH-

189   1 (*ndhD1D2*), acetate kinase (*ackA*), and PHB synthase (*phaEC*) (Table 1)*.* These

190   additional targets were predicted to enhance butanol synthesis.[26,27] The arrays were

191   used to make KS142 and KS143, containing sgRNA_*gltA*_463 and sgRNA_*gltA*_762,

192   respectively. KS142 and KS143 also contained the soluble transhydrogenase Sth

193   from *P. aeruginosa* (Fig. S6).[28] KS87 served as a control strain as it contained an

194   sgRNA array lacking *gltA* repression but was otherwise identical (Table 1).

195   We tested the growth and butanol production of the partial repression

196   strains in a photobioreactor under a batch "photonfluxostat" regime, where the light

197   intensity/OD is constant. This setup is intended to extend the exponential growth

198   phase and allows more accurate calculation of specific productivity.[23] We found that

199   growth of the three strains was not significantly different, indicating that *gltA*

200   repression was not severe (Fig. 4A). In KS142 (*gltA*_463), specific butanol

201   productivity (white bars in Fig. 4B) and butanol titers (Fig. 4C) were significantly

202   higher than in KS87. In KS143 (*gltA*_762), butanol titers were significantly higher

than KS87, but specific productivity was not (two-way repeated measures ANOVA, p<0.05). Over the 4-day measurement period, carbon partitioning to butanol was on average 16% in KS142 (*gltA*_463), 11% for KS143 (*gltA*_762), and 9% for KS87 (*no sgRNA_gltA*) (Fig. 4B and Supplementary Note). Quantitative PCR of *gltA* mRNA levels showed that *gltA* was repressed 11% in KS142 and 15% in KS143, though the differences between the two strains were within the margin of error of the qPCR assay (Fig. S7). These results show that partial repression of *gltA* can increase butanol titers without affecting growth.
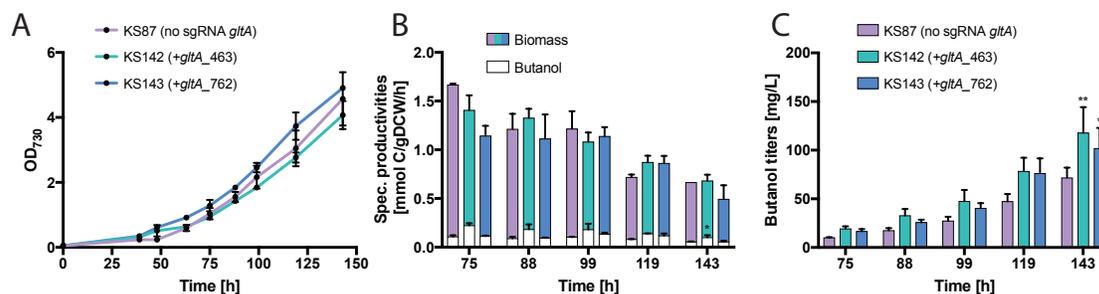
Figure 4. Carbon partitioning from biomass formation to butanol formation by partial repression of *gltA*. (A) Growth curve, (B) carbon partitioning, and (C) butanol titers. White bars in panel B indicate flux going to butanol whereas colored bars indicate flux going to biomass in C-mmol/gDCW/h. CRISPRi was induced with aTc in a pre-culture 4 days prior to experiment start. Strains were cultivated in the multicultivator in "photonfluxostat" mode with a light regime of 900 µmol photons m^{-2} s^{-2} OD_{720}^{-1}. Cultures were grown in duplicate. Two-way repeated measures ANOVA are denoted (* $p<0.05$; ** $p<0.005$).

We have shown that CRISPRi can be used as an effective tool to partition carbon flux between biomass and product in *Synechocystis.* Targeted repressions that affected metabolic branch points *and* arrested growth at an optimal cell density gave higher biofuel titers. Future efforts on two-phase production should focus on how to maintain a high CO_2 uptake and cell metabolism while growth is arrested. For instance, glucose uptake was improved in nitrogen-limited *E. coli* by modulating

226 the stringent response program, in effect removing the growth arrest signal.[29] A

227 high substrate uptake must also be maintained over extended time periods to make

228 two-stage fermentation processes successful.[30] The future success of growth-

229 arrested strains will thus depend on understanding the mechanisms underlying

230 decreased metabolic activity. For *Synechocystis*, one result of growth arrest is the

231 accumulation of NADPH from the light reactions that is not used in biomass

232 formation. Accumulation of NADPH could lead to a more reduced PQ pool,[31] which

233 causes photo-inhibition and thus reduced CO_2 fixation. If the biofuel pathway does

234 not carry enough flux, or does not utilize NADPH, reductant-dissipation valves may

235 be necessary. An additional line of evidence supporting this is our observation that

236 butanol-producing cultures, which generally carried less flux to product, became

237 bleached earlier after the onset of growth repression than ethanol-producing

238 cultures.

239 In this study, we have induced growth arrest via addition of an external

240 inducer. In the future, both CRISPRi and pathways for biofuel production could be

241 triggered by environmental signals, such as cellular density,[32] precursor

242 accumulation,[33] light or nitrate concentration.[34] Fine-tuning a light-intensity circuit

243 response[35] could ensure that growth suppression would occur when cell density is

244 optimal. Cyanobacteria can also react to different light colors[36] and future indoor

245 processes using LED lights[37] could involve switching light color to trigger

246 production phase. Such a true "dynamic engineering" approach would also require a

247 shorter delay time than reported here, likely through faster degradation of GltA

248 once transcription is blocked.

250 **Methods**

251

252 *Cyanobacteria cultivation*

253 For the flask cultivations, mutant *Synechocystis* sp. PCC 6803 strains were cultivated

254 at 30°C in a climatic chamber (Percival Climatics SE-1100), 100 µE/s/m^2

255 illumination, and 1 % v/v CO_2. Cultures were grown in BG-11 buffered to pH 7.8 and

256 supplemented with the appropriate antibiotics. IPTG (1mM), to induce expression of

257 nphT7, was added at OD_{730} 0.4. Induction of dCas9 and sgRNAs was with aTc added

258 to 1µg/mL at OD_{730} 0.1 unless specified. Additional aliquots of aTc were added every

259 two days. The multicultivator (Photon Systems Instruments) was run either in batch

260 mode or 'photonfluxostat' (light regime factor 900 µmol photons m^{-2} s^{-2} OD_{720}^{-1}).[23]

261 CO_2 from the outlet was measured online using a Cozir CM-0124 CO_2 sensor

262 (CO2Meter.com). The CO_2 concentration difference between outlet and inlet and gas

263 flow rate was used to calculate CO_2 uptake rate.

264

265 *Constructs and strains*

266 *Synechocystis* sp. PCC 6803 was a gift from Dr. Martin Fulda (Göttingen, Germany).

267 All genes, promoters, terminators, and antibiotic resistance cassettes were

268 assembled using Biobrick assembly. Biofuel production pathways were inserted at

269 the *slr0168* locus (NSI), dCas9 at the *psbA2* (NSII) locus and the sgRNAs at the

270 *slr2030* (NSIII) locus using pMD19-T targeting vector backbone (Takara). Strain

271 genotypes were verified by colony PCR. A list of strains used for this study is

272 available (Table 1 and Table S1).

273

274 *Butanol and ethanol measurement*

275 Cultures were pelleted at 13000 rpm for 10 min at 4°C. For butanol, 300 µL

276 supernatant was mixed vigorously with 100 µL dichloromethane for 30 s.

277 Isobutanol (5 µL, 0.1%) was used as internal standard. For ethanol, 80 µL

278 supernatant was mixed with 80 µL acetonitrile. Butanol (10 µL, 0.1%) was used as

279 internal standard. Both ethanol and butanol were quantified through GC-FID

280 (Shimadzu GC2010 Plus) using a Stabilwax column (30 m x 0.25 mm ID, 0.25 µm

281 film thickness, RESTEK).

282

283 *Minimization of Metabolic Adjustment (MOMA)*
284
285 We used an updated version[26] of the iJN678 genome-scale model.[19] Minimization of

286 metabolic adjustment (MOMA) was performed using the OptFlux software[38] to

287 predict flux distributions of mutant strains.[39] FBA was performed using the COBRA

288 toolbox 2.0[40] on MATLAB (Mathworks Inc.).

289

290 *Design of sgRNAs*

291 We used an in-house Python script to find potential sgRNAs inside a given ORF. The

292 algorithm made sure to select sgRNAs without unwanted off-target bindings,

293 absence of Biobrick restriction sites in the sequence, absence of terminators, as well

294 as additional stability criteria. A list of sgRNAs used in this study is available in the

295 supplemental (Table S2).

296

297 *RT-qPCR*

298   Total RNA was isolated from 4 mL of *Synechocystis* culture (OD_{730} = 1.0-3.0) using

299   the GeneJet RNA purification kit (Thermo Fisher). Manufacture's instructions were

300   followed except that lysozyme was added to the TE buffer to 40 mg/L instead of 0.4

301   mg/L. Beads were also used to lyse the cells. DNA was removed using the RapidOut

302   DNA Removal Kit (Thermo Fisher). RT-qPCR was performed on 50–100 ng of total

303   RNA with the Power SYBR Green RNA-to-Ct kit (Thermo Fisher) and a BioRad CFX

304   light cycler. Reference gene *rpoB* (*sll1787*) was used as internal standard.

305   Appropriate no-RT controls were also included.

306

307   *NADPH quantification*

308   Cultures (10ml) were pelleted at 4000 g for 10 min at 4°C. The pellets were

309   resuspended in 200 μL cold 0.2 M NaOH + 1 % (w/V) DTAB. Glass beads were added

310   (100 μL), samples were vortexed for 30 min at 4°C and centrifuged at 13000 rpm for

311   10 min at 4°C. The supernatants were analysed with the NADP/NADPH-Glo Assay

312   Kit (Promega) according to the manufacturer's protocol.

313

314   **Supporting Information:** A file containing supplementary table and figures (PDF).

315

316   **Author contributions**

317   KS and EPH proposed the idea, designed the experiments and wrote the paper. KS

318   and EL performed the experiments. JA designed the butanol pathway and

319   established product quantification. MJ set up the multicultivator and CO_2 sensors. LY

320   provided the dCas9 strains. EPH supervised. All authors read and approved the final

321   manuscript.

322

323   The authors declare no financial competing interest.

324

329

330   **References**
331   (1) Brockman, I. M., and Prather, K. L. J. (2015) Dynamic metabolic engineering: New
332   strategies for developing responsive cell factories. *Biotechnol. J 10*, 1360–1369.
333   (2) Venayak, N., Anesiadis, N., Cluett, W. R., and Mahadevan, R. (2015) Engineering
334   metabolism through dynamic control. *Curr. Opin. Biotechnol. 34*, 142–152.
335   (3) Lynch, M. D. (2016) Into new territory: Improved microbial synthesis through
336   engineering of the essential metabolic network. *Curr. Opin. Biotechnol. 38*, 106–111.
337   (4) Cho, H. S., Seo, S. W., Kim, Y. M., Jung, G. Y., and Park, J. M. (2012) Engineering
338   glyceraldehyde-3-phosphate dehydrogenase for switching control of glycolysis in
339   escherichia coli. *Biotechnol. Bioeng. 109*, 2612–2619.
340   (5) Soma, Y., Tsuruno, K., Wada, M., Yokota, A., and Hanai, T. (2014) Metabolic flux
341   redirection from a central metabolic pathway toward a synthetic pathway using a
342   metabolic toggle switch. *Metab. Eng. 23*, 175–184.
343   (6) Brockman, I. M., and Prather, K. L. J. (2015) Dynamic knockdown of E. coli central
344   metabolism for redirecting fluxes of primary metabolites. *Metab. Eng. 28*, 104–113.
345   (7) Yuan, J., and Ching, C. B. (2015) Dynamic control of ERG9 expression for
346   improved amorpha-4,11-diene production in Saccharomyces cerevisiae. *Microb. Cell
347   Fact. 14*, 1–10.
348   (8) Li, S., Jendresen, C. B., Grünberger, A., Ronda, C., Jensen, S. I., Noack, S., and
349   Nielsen, A. T. (2016) Enhanced protein and biochemical production using CRISPRi-
350   based growth switches. *Metab. Eng. 38*, 274–284.
351   (9) Straka, L., and Rittmann, B. E. (2017) Effect of culture density on biomass
352   production and light utilization efficiency of Synechocystis sp. PCC 6803. *Biotechnol.
353   Bioeng. 115*, 507–511.
354   (10) Kopka, J., Schmidt, S., Dethloff, F., Pade, N., Berendt, S., Schottkowski, M., Martin,
355   N., Dühring, U., Kuchmina, E., Enke, H., Kramer, D., Wilde, A., Hagemann, M., and
356   Friedrich, A. (2017) Systems analysis of ethanol production in the genetically
357   engineered cyanobacterium Synechococcus sp. PCC 7002. *Biotechnol. Biofuels 10*, 56.
358   (11) Yao, L., Cengic, I., Anfelt, J., and Hudson, E. P. (2016) Multiple Gene Repression
359   in Cyanobacteria Using CRISPRi. *ACS Synth. Biol. 5*, 207–212.

360 (12) Gordon, G. C., Korosh, T. C., Cameron, J. C., Markley, A. L., Begemann, M. B., and
361 Pfleger, B. F. (2016) CRISPR interference as a titratable, trans-acting regulatory tool
362 for metabolic engineering in the cyanobacterium Synechococcus sp. strain PCC
363 7002. *Metab. Eng. 38*, 170–179.
364 (13) Kaczmarzyk, D., Cengic, I., Yao, L., and Hudson, E. P. (2018) Diversion of the
365 long-chain acyl-ACP pool in Synechocystis to fatty alcohols through CRISPRi
366 repression of the essential phosphate acyltransferase PlsX. *Metab. Eng. 45*, 59–66.
367 (14) Huang, C. H., Shen, C. R., Li, H., Sung, L. Y., Wu, M. Y., and Hu, Y. C. (2016) CRISPR
368 interference (CRISPRi) for gene regulation and succinate production in
369 cyanobacterium S. elongatus PCC 7942. *Microb. Cell Fact. 15*, 196.
370 (15) Anfelt, J., Kaczmarzyk, D., Shabestary, K., Renberg, B., Uhlen, M., Nielsen, J., and
371 Hudson, E. P. (2015) Genetic and nutrient modulation of acetyl-CoA levels in
372 Synechocystis for n-butanol production. *Microb. Cell Fact. 14*, 167.
373 (16) Lan, E. I., and Liao, J. C. (2012) ATP drives direct photosynthetic production of
374 1-butanol in cyanobacteria. *Proc. Natl. Acad. Sci. 109*, 6018–6023.
375 (17) Heo, M. J., Jung, H. M., Um, J., Lee, S. W., and Oh, M. K. (2017) Controlling Citrate
376 Synthase Expression by CRISPR/Cas9 Genome Editing for n-Butanol Production in
377 Escherichia coli. *ACS Synth. Biol. 6*, 182–189.
378 (18) Koropatkin, N. M., Pakrasi, H. B., and Smith, T. J. (2006) Atomic structure of a
379 nitrate-binding protein crucial for photosynthetic productivity. *Proc. Natl. Acad. Sci.*
380 *103*, 9820–9825.
381 (19) Nogales, J., Gudmundsson, S., Knight, E. M., Palsson, B. O., and Thiele, I. (2012)
382 Detailing the optimality of photosynthesis in cyanobacteria through systems biology
383 analysis. *Proc. Natl. Acad. Sci. 109*, 2678–2683.
384 (20) Huang, H.-H., and Lindblad, P. (2013) Wide-dynamic-range promoters
385 engineered for cyanobacteria. *J. Biol. Eng. 7*, 10.
386 (21) Landry, B. P., Stöckel, J., and Pakrasi, H. B. (2013) Use of degradation tags to
387 control protein levels in the cyanobacterium Synechocystis sp. strain PCC 6803.
388 *Appl. Environ. Microbiol. 79*, 2833–2835.
389 (22) Albers, E., Larsson, C., Andlid, T., Walsh, M. C., and Gustafsson, L. (2007) Effect
390 of nutrient starvation on the cellular composition and metabolic capacity of
391 Saccharomyces cerevisiae. *Appl. Environ. Microbiol. 73*, 4839–4848.
392 (23) Du, W., Jongbloets, J. a., Pineda Hernãndez, H., Bruggeman, F. J., Hellingwerf, K.
393 J., and Branco dos Santos, F. (2016) Photonfluxostat: A method for light-limited
394 batch cultivation of cyanobacteria at different, yet constant, growth rates. *Algal Res.*
395 *20*, 118–125.
396 (24) Ducat, D. C., Avelar-Rivas, J. A., Way, J. C., and Silver, P. A. (2012) Rerouting
397 carbon flux to enhance photosynthetic productivity. *Appl. Environ. Microbiol. 78*,
398 2660–2668.
399 (25) Qi, L. S., Larson, M. H., Gilbert, L. A., Doudna, J. A., Weissman, J. S., Arkin, A. P.,
400 and Lim, W. A. (2013) Repurposing CRISPR as an RNA-guided platform for
401 sequence-specific control of gene expression. *Cell 152*, 1173–1183.
402 (26) Shabestary, K., and Hudson, E. P. (2016) Computational metabolic engineering
403 strategies for growth-coupled biofuel production by Synechocystis. *Metab. Eng.*
404 *Commun. 3*, 216–226.
405 (27) Erdrich, P., Knoop, H., Steuer, R., and Klamt, S. (2014) Cyanobacterial biofuels:

406   new insights and strain design strategies revealed by computational modeling.
407   *Microb. Cell Fact. 13*, 128.
408   (28) Angermayr, S. A., Paszota, M., and Hellingwerf, K. J. (2012) Engineering a
409   cyanobacterial cell factory for production of lactic acid. *Appl. Environ. Microbiol. 78*,
410   7098–7106.
411   (29) Michalowski, A., Siemann-herzberg, M., and Takors, R. (2017) Escherichia coli
412   HGT : Engineered for high glucose throughput even under slowly growing or resting
413   conditions. *Metab. Eng. 40*, 93–103.
414   (30) Klamt, S., Mahadevan, R., and Hädicke, O. (2017) When Do Two-Stage Processes
415   Outperform One-Stage Processes ? *Biotechnol. J. 13*.
416   (31) Keren, N., and Krieger-Liszkay, A. (2011) Photoinhibition: Molecular
417   mechanisms and physiological significance. *Physiol. Plant. 142*, 1–5.
418   (32) Basu, S., Mehreja, R., Thiberge, S., Chen, M.-T., and Weiss, R. (2004)
419   Spatiotemporal control of gene expression with pulse-generating networks. *Proc.
420   Natl. Acad. Sci. 101*, 6355–60.
421   (33) Rogers, J. K., Taylor, N. D., and Church, G. M. (2016) Biosensor-based
422   engineering of biosynthetic pathways. *Curr. Opin. Biotechnol. 42*, 84–91.
423   (34) Immethun, C. M., DeLorenzo, D. M., Focht, C. M., Gupta, D., Johnson, C. B., and
424   Moon, T. S. (2017) Physical, Chemical, and Metabolic State Sensors Expand the
425   Synthetic Biology Toolbox for Synechocystis sp. PCC 6803. *Biotechnol. Bioeng. 114*,
426   1561–1569.
427   (35) Ang, J., Harris, E., Hussey, B., Krill, R., and McMillen, D. R. (2013) Tuning
428   Biological Response Curves for Synthetic Biology. *ACS Synth. Biol. 2*, 547–567.
429   (36) Chau, R. M. W., Bhaya, D., and Huang, K. C. (2017) Emergent phototactic
430   responses of cyanobacteria under complex light regimes. *MBio 8*, 1–15.
431   (37) Lips, D., Schuurmans, J. M. M., Branco dos Santos, F., and Hellingwerf, K. J.
432   (2017) Many ways towards "solar fuel": Quantitative analysis of the most promising
433   strategies and the main challenges during scale-up. *Energy Environ. Sci. 11*, 10–22.
434   (38) Rocha, I., Maia, P., Evangelista, P., Vilaça, P., Soares, S., Pinto, J. P., Nielsen, J.,
435   Patil, K. R., Ferreira, E. C., and Rocha, M. (2010) OptFlux: an open-source software
436   platform for in silico metabolic engineering. *BMC Syst. Biol. 4*, 45.
437   (39) Segrè, D., Vitkup, D., and Church, G. M. (2002) Analysis of optimality in natural
438   and perturbed metabolic networks. *Proc. Natl. Acad. Sci. 99*, 15112–15117.
439   (40) Schellenberger, J., Que, R., Fleming, R. M., Thiele, I., Orth, J. D., Feist, A. M.,
440   Zielinski, D. C., Bordbar, A., Lewis, N. E., Rahmanian, S., Kang, J., Hyduke, D. R., and
441   Palsson, B. O. (2011) Quantitative prediction of cellular metabolism with constraint-
442   based models: the COBRA Toolbox. *Nat. Protoc. 6*, 1290–1307.
443
444